INCREMENT OF TRAINING SANPLES FOR SUPERVISED HYPERSPECTRAL CLASSIFICATION BASED ON SPECTRAL SIMILARITY

Masamitsu Ochiai, Yukio Kosugi, Kuniaki Uto

Interdisciplinary Graduate School of Science and Engineering, Tokyo Institute of Technology
E-mail: ochiai.m.ac@m.titech.ac.jp

KEY WORDS: Remote Sensing, hyperspectral image, semi-supervised classification, land use classification, region growing

Abstract: A hyperspectral image has a data structure including rich information, widely used for remote sensing techniques. A lot of classification techniques for the image are studied, and especially supervised classification techniques show high accuracy. However, supervised techniques classify hyperspectral images with law accuracy, with little number of training samples. In this study, a method increasing the number of training samples using spatial and spectral information is proposed to improve supervised hyperspectral classification accuracy. Experimental results are presented for a synthetic hyperspectral image and a real hyperspectral image, i.e. the Takasaka Farm Image acquired by CASI sensor over the farm in Yamagata, Japan. In a test on a synthetic data, efficacy of the proposed approach is proved. In addition, in a test on Takasaka Farms Image, the number of training samples was increased from 40 to 31,188, and in SVM classification results, overall accuracy increased from 77.72% to 92.27%.

1. INTRODUCTION

Hyperspectral images have a structure including rich information and are widely used for remote sensing techniques. Acquired by Airborne or spaceborne sensors, hyperspectral images are composed of hundreds of images corresponding to each of observed channel. This rich information increases the capability to distinguish different physical materials in the image. Thus, it is effective to classify collected imagery into distinct material constituents relevant to particular application, and produce classification maps that indicate where the constituents are present. This process contributes essential information to landcover maps for environmental remote sensing, surface mineral maps for geological applications and precious mineral exploration, vegetation species for agricultural or other earth science studies, or manmade materials for urban mapping. However, the hyperspectral classification process isn't so simple due to characteristic problems which come from the rich information of the hyperspectral image, such as the curse of dimensionality.

Recently, a lot of classification techniques are studied. At present, as compared to supervised ones, high precision classification result hasn't been acquired by unsupervised classification techniques, primarily due to the inherent ambiguity that exists in the way in which non-normal data distribution can be statistically represented. On the other hands, supervised techniques, in particular, using kernel-based methods or support vector machines (SVMs), have successfully revealed better accuracy in hyperspectral image classification. In addition, new techniques such that the existing pixel-wise supervised classification techniques are combined with spatial information acquired from the image are studied, which increase classification accuracy by declining the number of pixel-wise misclassifications, mainly estimating an outline of each object in the image, or merging a pair of spatially adjoining pixels being spectrally near. However, in these techniques, a lot of training samples are required, and when little number of training samples are available, high classification accuracy isn't achieved because the underlying data distribution is not properly captured.

In this paper, a new preprocessing approach for supervised hyperspectral classification is proposed, which improves supervised hyperspectral classification accuracy with little number of training samples by increasing the number of training samples, using spatial and spectral information. In this process, spatial continuity and spectral similarity in each constituent's class are assumed. Experimental results are demonstrated on a synthetic hyperspectral image, and a real hyperspectral airborne image recorded by the Compact Airborne Spectrographic Imager (CASI) over the Takasaka farm of Yamagata prefecture, Japan.

2. SPECTRALLY-SPATIALLY INCREASING TRAINING SAMPLES

In the proposed approach, it is assumed that spectra in the same class are similar to each other. In addition, all spatial objects in an image are composed of one or several pixels, and these pixels in the same object belong to the same class. Thus, spatial continuity of pixels in the same class is assumed. Some labeled pixels in an image are

given as training samples. Using them, unlabeled pixels in the image would be labeled as a new training sample. The process is specified in the following section.

2.1. Region Growing with Adjoining Pixel's Similarity

Dissimilarity criterion values between labeled pixels and the adjoining unlabeled ones are calculated by the standard Spectral Angle Mapper (SAM). The SAM measure between u_i and u_j (u_i, $u_j \in R^B$) determines the spectral similarity between two vectors by computing the angle between them.

$$\mathrm{SAM}(u_i, u_j) = \arccos\left(\frac{\sum_{b=1}^{B} u_{ib}u_{jb}}{\left[\sum_{b=1}^{B} u_{ib}^2\right]^{1/2}\left[\sum_{b=1}^{B} u_{jb}^2\right]^{1/2}}\right) \quad (1)$$

where B is the number of bands, $u_i=\{u_{i1},\ldots,u_{iB}\}^T$ and $u_j=\{u_{j1},\ldots,u_{jB}\}^T$ are reflectance vectors corresponding data index i and j.

A pair having smallest SAM value is selected, and an unlabeled pixel of the pair is labeled same as the other labeled one. This process is repeated until there is no pair whose SAM value is under threshold.

2.2. Robust Color Morphological Gradient (RCMG)

Aforementioned process is considered as region growing from labeled pixels, taken as seeds of the regions. This approach is based on spectral similarity and pixel's spatial continuity in the same class. However, when the process is applied and adjoining similar pixels are captured in a certain region, some pixels belonging to other classes could be captured too, in case they are similar to and adjoin the region. In addition, in a case when two objects constructed of different similar constituents spatially adjoin each other in an image, a region could grow beyond a boundary of the objects and some pixels in each object could be labeled the same.

To avoid that, spatial gradient of pixels in the image is considered in the proposed approach. Regions are prevented from growing beyond object's boundaries by being prohibited to grow in directions where a value of gradient increases, because there are any large spectral difference like an object's boundary in an area having a large amount of gradient. The gradient is calculated by using a robust color morphological gradient (RCMG).

For each pixel vector x_p, let $X = [x_p^1, x_p^2, \ldots, x_p^e]$ be a set of e vectors contained within a structure element E. The RCMG, using the Euclidian distance, is defined as

$$RCMG_E(x_p) = \max_{i,j\in[X-REM_r]}\left\{\left\|x_p^i - x_p^j\right\|_2\right\} \quad (2)$$

where REM_r is a set of r furthest apart vector pairs in E removed to avoid the effect of outliers. By calculating RCMG, each pixel in the image is given a value representing if there is any pairs of pixels having huge spectral distance nearby. If there is a pair like that around a certain pixel, the pixel is given a high RCMG value. In the proposed approach, unless RCMG is less than a given threshold, regions are prohibited from growing in directions where RCMG increases. It prevents regions from growing to spatially enter other object's space constructed of different constituents and grow within the space.

2.3. Evaluation with Class Mean Vectors

In the process described above, the number of training samples is increased by region growing from pixels initially labeled as training samples. In addition, it is prevented for regions to spatially enter from one object to another beyond a boundary. However, in case there is a boundary having relatively too little RCMG (it means the boundary is of relatively too similar objects), a region could grow beyond the boundary, because regions grow in direction where RCMG value increase unless the value beyond threshold. To avoid that, when an unlabeled pixel x^* satisfies aforementioned condition and is labeled as a training sample of the class C, SAM between it and a class mean vector is calculated per each class. If the SAM value between x^* and a class mean vector of the class C is smaller than the others' SAM value, the pixel x^* is permitted to be labeled as a training sample of the class C. By this process, it is possible to avoid regions growing beyond boundaries having relatively smaller RCMG.

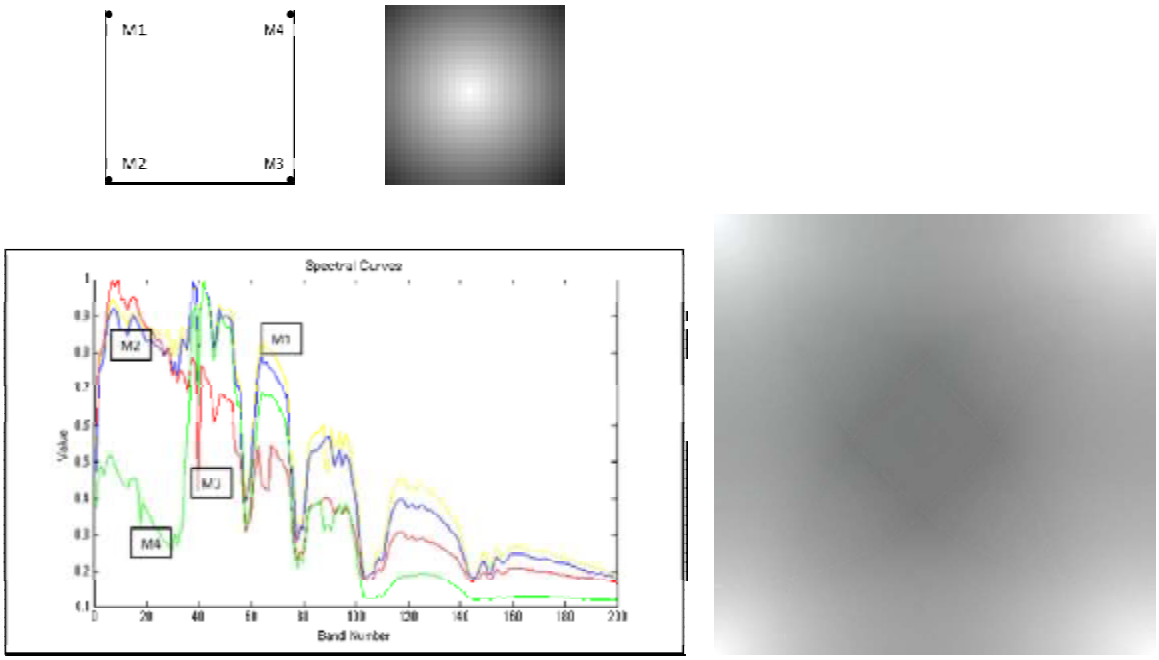

(a) **(d)**

Figure 1: Synthetic Hyperspectral Data

It is assumed that within-class variances of SAM values are identical here. Though the difference of the variances should be considered, it is difficult to predict correct amount of the variance in each class, especially in case there is little number of training samples is assumed.

3. EXPERIMENTAL RESULTS

Two different images were used for the experiments. One of them is a synthetic image and the other is a real image, acquired by CASI airborne imaging spectrometers. These images and the corresponding results are presented in the next two sections.

3.1 Experiment 1: Synthetic Hyperspectral Image

A synthetic hyperspectral image, simulated with the four pure spectral signatures in Fig.1 (a), was used for a test of proposed approach. The image was simulated by assuming that the pixels located at the 4 pixels (M1-M4 in Fig.1 (b)) of an image circle consist of 100% abundance, with their immediate neighboring pixels made up of linearly reduced abundance fractions, until a fraction of 0% is simulated outside the imaginary circle (see Fig.1 (c)). Where some of the circles are overlapped, the spectra are mixed (Fig.1 (d)). The size of the image is 30 by 30 pixels, and a radius of the circles is 25 pixels.

To the image, a proposed approach was applied in four patterns for comparison, only adjoining pixel's SAM were used (Fig.2 (i)), adjoining pixel's SAM and RCMG value were used (Fig.2 (ii)), adjoining pixel's SAM and class mean SAM were used (Fig.2 (iii)), and all of three values were used (Fig.2 (iv)). A pixel located at a center of each circle was used for an initial training sample for each class, and used for the proposed approach. In each patterns, threshold of adjoining pixel's SAM was set to mean value of the SAM of all pairs in the image (Fig.2 (a)), it added to standard deviation of the SAM of all pairs in the image (Fig.2 (b)), and it added to double amount of the standard deviation (Fig.2 (c)).

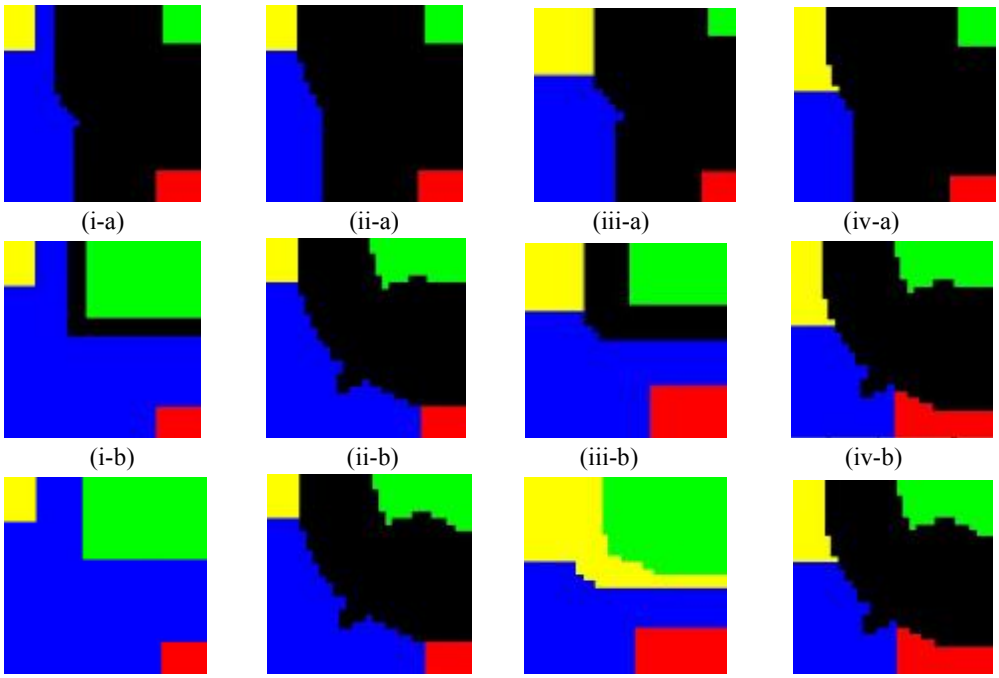

Figure 2: Synthetic hyperspectral image. (i) Only adjoining pixel's SAM are calculated. (ii) Adjoining pixel's SAM and RCMG are calculated. (iii) Adjoining pixel's SAM and SAM with class mean vectors are calculated. (iv) All of three values are calculated. From (a) to (c), different thresholds of adjoining pixel's SAM are used. (a) A mean value of the SAM of all pairs in the image. (b) A sum of standard deviation of the SAM of all pairs in the image and the threshold of (a). (c) A sum of twofold standard deviation of the SAM of all pairs in the image and threshold of (a).

Table 1: Result for the Takasaka Farm image. Number of labeled samples in reference data (No. of samples), Number of increased training samples (No. of increased TS), Number of increased training samples labeled in a reference data (No. of increased TS known correct label), Accuracy of increased training samples calculated with a reference data, ignoring ones unlabeled in a reference data (Accuracy of increased TS), SVM classification accuracy with training samples before increased (SVM by former TS), and after increased by the proposed approach (SVM by increased TS)

	No. of samples	No. of increased TS	No. of increased TS known correct label	Accuracy of increased TS	SVM by former TS	SVM by increased TS
OA				100	77.72	**92.27**
AA				100	78.74	**84.59**
κ				100	71.69	**89.83**
Leaf of apple	1317	536	63	100	**67.50**	48.60
Leaf of cherry blossom	1685	87	76	100	**65.52**	58.34
Leaf of chestnut	4846	1307	1182	100	65.74	**90.78**
Leaf of persimmon	247	413	166	100	84.21	**97.17**
Leaf of grape and soil	5804	2846	2660	100	42.61	**96.55**
Paddy	12347	5386	5023	100	94.99	**100**
Soil	1810	24	22	100	**90.55**	84.64
Soil through plastic	609	229	229	100	94.91	**97.04**
Concrete	2458	19	18	100	96.75	**97.36**
Bldg	65	7	7	100	**84.62**	75.38

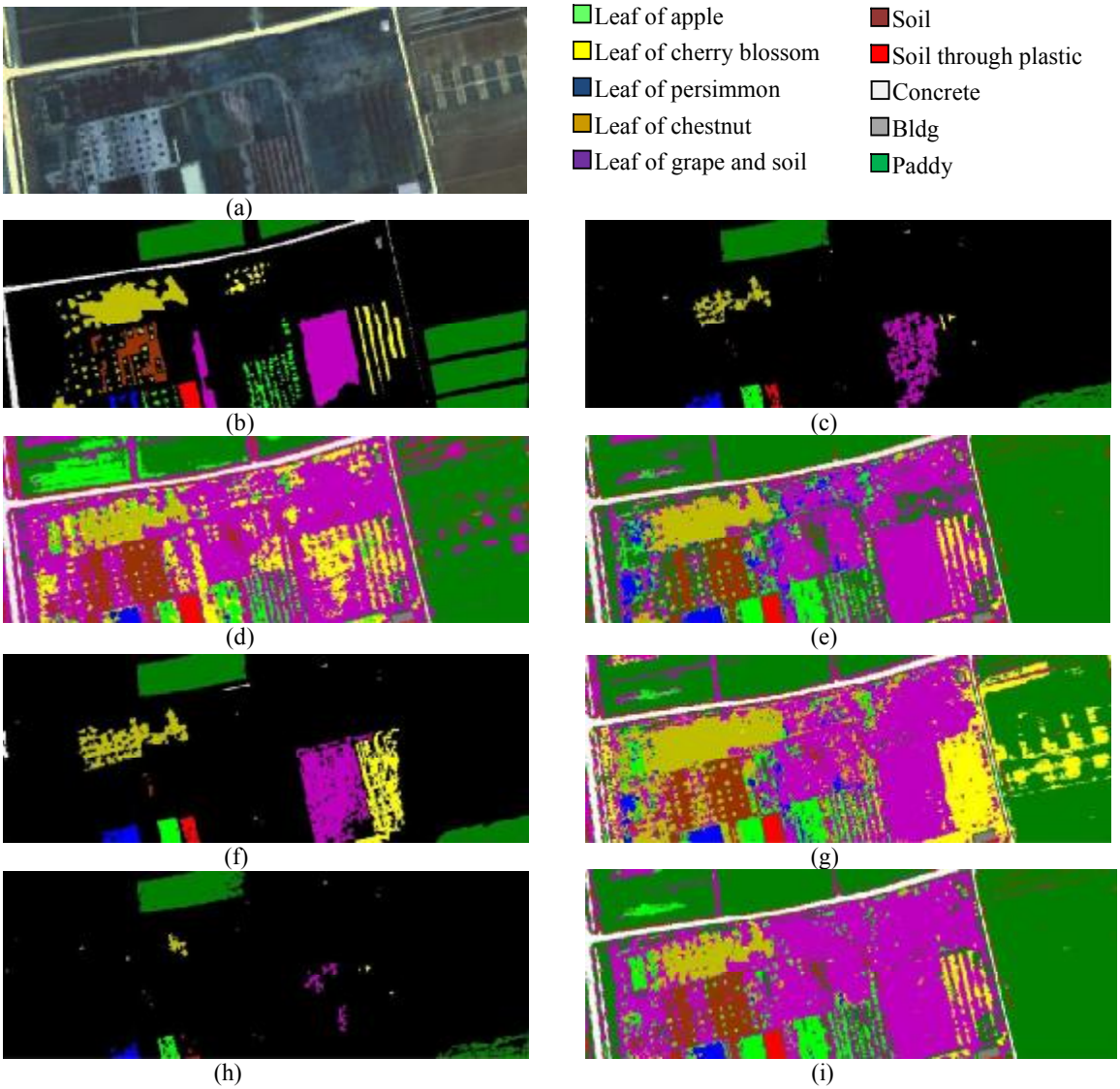

Figure 3: Takasaka farm image. (a) Tree-band color composite. (b) Reference map. (c) Increased training samples (TS) map. (d) SVM classification map with original TS. (e) SVM classification map with TS of (c). (f) Increased TS with lower threshold. (g) SVM classification map with TS of (f). (h) Increased TS with higher threshold. (i) SVM classification map with TS of (h).

By comparison of Fig.2 (i) with Fig.2 (ii) (even the same as Fig.2 (iii) and Fig.2 (iv)), it is shown that regions grow around boundaries between dissimilar objects (M1-M2-M3 and M4) only when RCMG is used. In addition, by comparison of Fig.2 (i) with Fig.2 (iii) (even the same as Fig.2 (ii) and Fig.2 (iv)), position of boundaries between grown regions, particularly M1 and M2 or M2 and M3, are clearly appropriate when class mean SAM is used.

3.2 Experiment 2: the Takasaka farm Image

The proposed approach is tested for a real image too. The Takasaka farm image is acquired by the CASI sensor over the Takasaka farm owned by the Yamagata University in Yamagata prefecture, Japan. The image has a size of 211 by 593 pixels, with a spatial resolution of 1.5 m/pixel. The number of data channels in the image is 67 (with a spectral range from 0.43 to 1.06 μm). 10 classes of interest are considered, detailed in Table.1, Fig.3, shows a three-

Table2: Result for the Takasaka Farm image with lower and higher threshold for the proposed approach. Number of increased training samples (No. of increased TS), Number of increased training samples labeled in a reference data (No. of increased TS known correct label), Accuracy of increased training samples calculated with a reference data, ignoring ones unlabeled in a reference data (Accuracy of increased TS), SVM classification accuracy for training samples after increased by the proposed approach (SVM by increased TS)

	Lower threshold				Higher threshold			
	No. of increased TS	No. of increased TS known correct label	Accuracy of increased TS	SVM by increase TS	No. of increased TS	No. of increased TS known correct label	Accuracy of increased TS	SVM by increase TS
OA			99.99	90.37			100	90.33
AA			99.99	85.23			100	84.03
κ			99.99	87.65			100	87.30
Leaf of apple	613	75	100	48.75	374	28	100	61.50
Leaf of cherry blossom	3214	824	99.88	78.04	35	32	100	58.69
Leaf of chestnut	2825	2342	100	95.73	243	228	100	72.68
Leaf of persimmon	589	212	100	97.17	258	108	100	89.88
Leaf of grape and soil	5938	4465	100	95.73	382	382	100	97.26
Paddy	5704	5256	100	90.59	4644	4331	100	100
Soil	62	55	100	87.46	23	21	100	88.84
Soil through plastic	393	393	100	94.91	46	46	100	95.57
Concrete	189	172	100	97.80	13	12	100	97.44
Bldg	7	7	100	66.15	7	7	100	78.46

band true color image and the reference data. Four pixels for each class were randomly chosen from the reference data as training samples. The classification accuracy of the proposed method is shown in Table.1.

In addition, each of original training samples and training samples increased by the proposed approach were used for the multiclass one versus one SVM classifier with the Gaussian radial basis function kernel parameters chosen by four-fold cross validation: in each classifier, a penalty parameter C is from 1024 to 8192, a width parameter γ of RBF-kernel is from 0.0156 to 0.1250. The classification accuracy is shown in Table.1.

From the Table.1, training samples were increased with a high accuracy by the proposed approach. However, many pixels which were unlabeled in the reference data were added to training samples too. As a result of each SVM classification using original training samples and training samples increased by proposed approach, OA, AA, κ were higher in classification using latter training samples.

On the other hand, some class's classification accuracies, especially "*Leaf of apple*" and "*Leaf of cherry blossom*", were lower in classification using training samples increased by the proposed approach. It is because relatively low number of training sample for these classes were captured even though these classes had many labeled pixels in a reference data, due to objects belonging to these classes narrowly spread spatially continuously, and scattered in the image.

The result of increased training samples when values of threshold were set lower is shown in Fig.3 (f), Table.2. In this case, increase of training samples in each class became larger, including more uncertain pixels for training samples which had a different label or unknown in a reference data. SVM classification result with these increased training samples is shown in Fig.3 (g), Table.2. Especially in "*Leaf of cherry blossom*" class, the classification accuracy became improved, due to a lot of training samples of the class was captured. However, the classification accuracy of other classes, especially "*Paddy*" class, was decreased. It might be affected by some pixels spatially located around objects of "*Leaf of cherry blossom*", labeled as the class's training samples even though they might belong to different classes.

On the other hand, when values of threshold were set higher, the result of increased training samples became as Fig.3 (h), Table.2. In this case, increase of each class's training samples became smaller, and there were less uncertain training samples in the increased ones. SVM classification result with these increased training samples is shown in Fig.3 (i), Table.2. In this classification result, "*Leaf of chestnut*" class's classification accuracy became especially less than the others, due to the number of the class's training samples were less than the others. However, because there is less difference of the number of training samples between classes, classification accuracy of "*Leaf of apple*" class is not much low with a little number of the class's training samples.

4. CONCLUSION

In this study, an approach increasing the number of training samples using spectral and spatial information is proposed to improve supervised hyperspectral classification accuracy with little number of training samples. In addition, efficacy of the proposed approach was shown by applying it to a synthetic hyperspectral image, and the approach was tested on a real hyperspecral image. It is shown that SVM classification accuracy was improved by increasing the number of training samples. However, some classes' training samples couldn't be captured much in case the class's objects were spatially scattered in an image. In the result, the classification accuracy of spatially scattered classes is lowered. To solve this problem, scattered objects belonging to the same class must be captured as training samples. Furthermore, not only increasing the number of training samples, but also selecting effective samples for classification must be done. Otherwise, training samples could be increased locally in probability density distribution of a class, and then the distribution of the classification result could be different from an ideal one.

REFERENCES:

H. Akbari and Y. Kosugi, "Hyperspectral imaging: a new modality in surgery," In-Tech pub, Recent Advances in Biomedical Engineering, pp. 223-240, 2009.

T. Asano, Y. Kosugi, K. Uto, N. Kosaka, S. Odagawa and K. Oda, "Leaf area index estimation from hyperspectral data using a group division method," Proc. IGARSS, 2009.

H. Akbari, Y. Kosugi, K. Kojima and N. Tanaka , "Detection and analysis of the intestinal ischemia using visible and invisible hyperspectral imaging," IEEE Trans. Biomedical Engineering, vol. 57, no. 8, pp. 2011-2017, Aug. 2010.

Y. Tarabalka, J. Chanussot, and J. A. Benediktsson, "Segmentation and classification of hyperspectral images using minimum spanning forest grown from automatically selected markers," IEEE Trans. Syst., Man, Cybern. B, Cybern., vol. 40, no. 5, pp. 1267-1279, Oct. 2010.

Y. Tarabalka, J. A. Benediktsson, J. Chanussot, and J. C. Tilton, "Multiple spectral-spatial classification approach for hyperspectral data," IEEE Trans. Geoscience and Remote Sensing., vol. 48, no. 11, pp. 4122-4132, Nov. 2010.

F. van der Meer, "The effectiveness of spectral similarity measures for the analysis of hyperspectral imagery," Int. J. Appl. Earth Observation Geoinformation, vol. 8, no. 1, pp. 3-17, 2006.

A. Evans and X. Liu, "A molphological and experimental analysis of linear combiners for multiple classifier systems," IEEE Trans. Image Process., vol. 15, no. 6, pp. 1454-1463, June. 2006.

G. Camps-Valls and L. Bruzzone, "Kernel-based methods for hyperspectral image classification," IEEE Trans. Geoscience and Remote Sensing., vol. 43, no. 6, pp. 1351-1362, June. 2005.

F. Melgani and L. Bruzzone, "Classification of hyperspectral remote sensing images with support vector machines," IEEE Trans. Geoscience and Remote Sensing., vol. 42, no. 8, pp. 1778-1790, Aug. 2004.

M. T. Eismann, "Hyperspectral remote sensing," SPIE Press Monograph, vol. PM210.